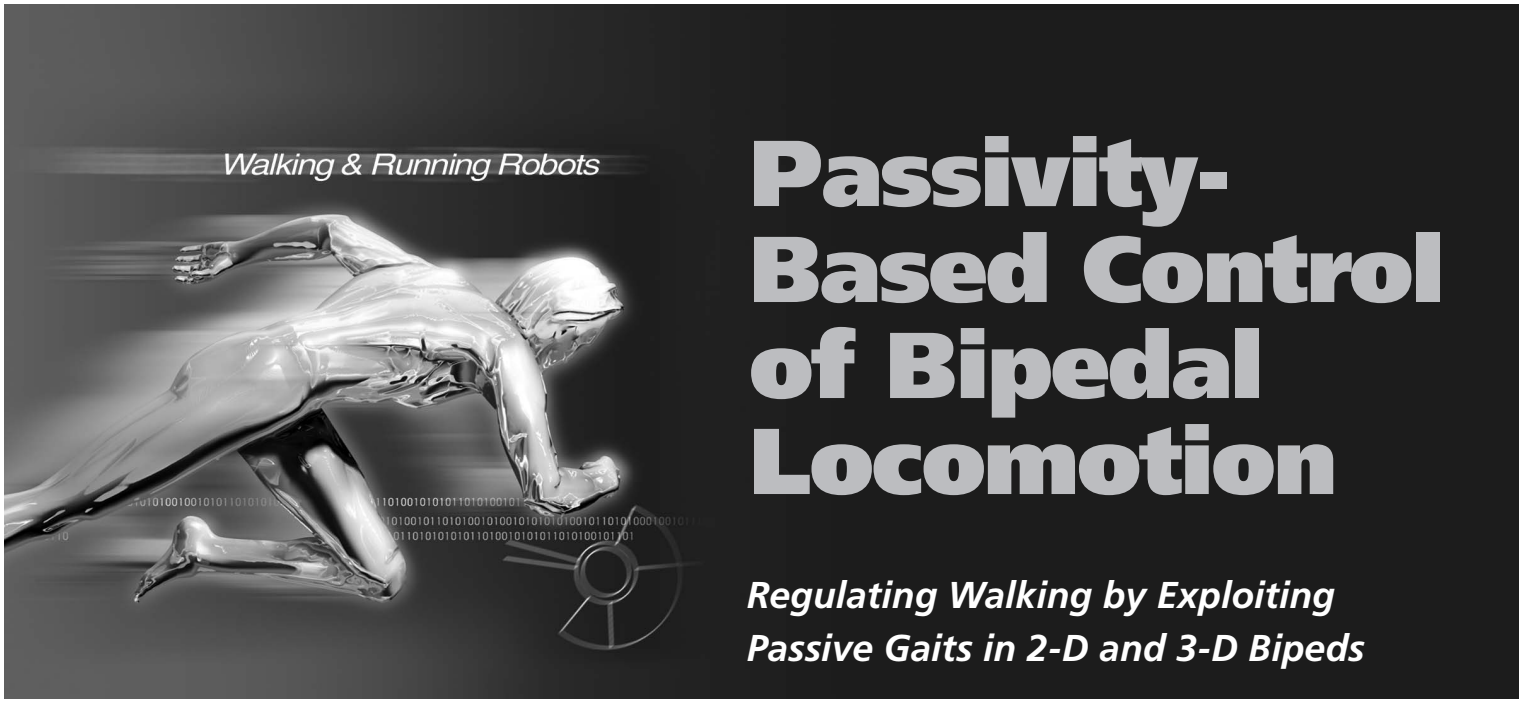

Passivity-Based Control of Bipedal Locomotion

Regulating Walking by Exploiting Passive Gaits in 2-D and 3-D Bipeds

This article is an overview of our recent results in passivity-based control in biped locomotion. The article represents a synthesis of ideas from [13], [27]–[32] into a set of cohesive results that exploits the notion of passive walking within the context of hybrid passivity-based control to achieve regulated walking on varying slopes, robustness to uncertainties and disturbances, as well as to regulate walking speed and gait transitions.

The idea of passive dynamic walking, pioneered by McGeer more than a decade ago [20], has been well studied by several researchers [6]–[8], [20] and will not be discussed here. We are interested primarily in active control methods that exploit the existence of passive gaits in two-dimensional (2-D) and three-dimensional (3-D) bipeds. While passive dynamic walking is appealing for its elegance and simplicity, active feedback control is necessary to achieve walking on level ground and varying slopes, robustness to uncertainties and disturbances, and to regulate walking speed. In this article, we show how to achieve these properties within the context of passivity-based control.

The first results in active feedback control that exploit passive walking appeared in [7], [22], [27], [28] for planar bipeds. Passive walking in three dimensions was studied in [17] and [4]. Later, the results in [28] were extended to the general case of 3-D walking in [31]. An interesting and elegant extension of these ideas appears in [1] where geometric reduction methods are used to generate stable 3-D walking from 2-D gaits. Robustness issues were addressed in [32] using total energy as a storage function in the hybrid passivity framework. In [13] it was shown how speed regulation, including gait transitions can be achieved within the context of passivity-based control.

The article is organized as follows. In the following section, we give the general background on hybrid Lagrangian models that are typically used to study bipedal locomotion and control. Then we discuss three central ideas in energy and passivity-based control of bipeds, namely, controlled symmetry [31], energy shaping [32], and trajectory time scaling [13]. Using these concepts we are able to show the following:

- how to generate stable gaits, i.e., limit cycle trajectories, on arbitrary ground slopes given a passive limit cycle on one particular slope
- how to increase both the size of the basin of attraction of the stable limit cycles and the speed of convergence to the limit cycles
- how to increase robustness of the closed-loop system to disturbances
- how to regulate forward walking speed and gait transitions.

To illustrate the performance of these controllers, we present simulation results for the so-called compass-gait biped. Finally, we give some suggestions for further research.

Dynamics of Bipedal Locomotion

In this section, we discuss the dynamics of bipedal locomotion. Our treatment will be necessarily brief as the hybrid Lagrangian model treated here has been developed and used extensively by numerous other researchers [1], [9], [14], [21]. See, for example, [34] for a detailed derivation of a general model in the planar case.

BY MARK W. SPONG, JONATHAN K. HOLM, AND DONGJUN LEE

1070-9932/07/$25.00©2007 IEEE

Configuration Space and Shape Variables

The act of walking involves both a swing phase and a stance phase for each leg as well as impacts between the swing leg and ground, and possibly internal impacts, such as knee strikes due to mechanical constraints on the joints. Consider an n degree-of-freedom (DoF) biped during the single-support phase as shown in Figure 1. Each joint of the robot is assumed to be revolute and to allow a single DoF rotation. The stance leg, which is in contact with the ground, has three DoF relative to an inertial frame (assuming no slipping). We can therefore use $Q = SO(3) \times \mathbb{T}^{n-3}$ to represent the configuration space of the biped, where $SO(3)$ is the rotation group in $\mathbb{R}^3$ and $\mathbb{T}^{n-3}$ is the $(n-3)$-torus. A configuration is then characterized by an ordered pair $q = (R, r)$, where $R \in SO(3)$ is the orientation of the first link and $r \in \mathbb{T}^{n-3}$ is the shape of the multibody chain, for example, the angle of each joint referenced to the previous joint. Given a configuration, $q = (R, r) \in SO(3) \times \mathbb{T}^{n-3}$, we represent a velocity vector in T_qQ via the pair $(R^{-1}\dot{R}, \dot{r}) \in \mathfrak{so}(3) \times \mathrm{R}^3$, where $\mathfrak{so}(3)$ is the Lie Algebra of 3×3 skew-symmetric matrices.

The advantage of this formalism is that only the orientation of the first link (actuated by the stance ankle) is referenced to an absolute or world frame. The remaining $n-3$ joint variables, called the shape variables, are then invariant under a change of basis of the world frame. Configuration spaces that can be written as the Cartesian product of a Lie group and a shape space are referred to as principal bundles; see [19].

Lagrangian Dynamics

To write the equations of motion for the walking biped during the single-support phase, it is common to introduce a parametrization of the configuration space $\mathrm{SO}(3) \times \mathbb{T}^{n-3}$, which is equivalent to $q = (R, r)$ but minimal, in the sense that only n coordinates are required. For example, we shall let $(q^1, \ldots, q^n)$ be a coordinate chart where (q^1, q^2, q^3) are Euler angles for $SO(3)$ and $(q^4, \ldots, q^n)$ are angles in $[0, 2\pi)$ for $\mathbb{T}^{n-3}$. Accordingly, we can write the Euler-Lagrange equations of motion as

$$\frac{d}{dt}\frac{\partial \mathcal{L}}{\partial \dot{q}^i} - \frac{\partial \mathcal{L}}{\partial q^i} = \sum_{j=1}^{n} B_{i,j}(q)u_j, \quad i = 1, \ldots, n, \qquad (1)$$

where $\mathcal{L}(q, \dot{q}) = \mathcal{K}(q, \dot{q}) - \mathcal{V}(q)$ is the difference of the kinetic energy $\mathcal{K} : TQ \to \mathbb{R}$ and the potential energy due to gravity, $\mathcal{V} : Q \to \mathbb{R}$, $B_{i,j}$ is the i-th component of the j-th force, which has magnitude u_j. If we express the kinetic energy in the usual fashion as $\mathcal{K}(q, \dot{q}) = \frac{1}{2}\dot{q}M(q)\dot{q}$, where $M(q)$ is the symmetric, positive definite $n \times n$ inertia matrix, the controlled Euler-Lagrange equations can be written in matrix form as [33]

$$M(q)\ddot{q} + C(q, \dot{q})\dot{q} + G(q) = B(q)u, \qquad (2)$$

where $\dot{M} - 2C$ is skew symmetric and $G(q) = d\mathcal{V}^T(q)$ is the vector of gravitational torques. We assume the walking biped is fully actuated so that the $n \times n$ matrix B in (2) is full rank for all q.

Impact Dynamics

Impacts arise in two ways: from the foot/ground contact and from internal constraints such as mechanical stops designed to prevent hyperextension of the knees. For space reasons, we analyze here only the impacts resulting from the foot/ground contact and we make some standard assumptions.

- Impacts are perfectly inelastic (no bounce).
- Transfer of support between swing and stance legs is instantaneous, i.e. the double support phase is negligible.
- There is no slipping at the foot/ground contact.

Under these assumptions, each impact results in an instantaneous jump in velocities, hence a discontinuity in kinetic energy, whereas the position variables are continuous through the impact (see [14]).

As a consequence of the second assumption, we also assume that the walking gait is flat-footed. In other words, we can define unambiguously a height function $H : Q \to \mathbb{R}$ defining the height of the swing leg above the ground. The foot/ground impact occurs, therefore, when $H = 0$ and $dH \cdot \dot{q} < 0$, the latter inequality guaranteeing that the foot velocity is directed toward the ground. In this way we avoid the case of heel strike–double support–toe off phases, which introduce subtleties beyond the scope of this article.

We denote by t^- and t^+ the times just prior to impact and just after impact, respectively. By instantaneous transfer of support, we mean not only that the swing leg and stance leg interchange roles at the moment of impact but also that the new stance leg lifts off the ground instantaneously, which can be expressed as $dH(q^-) \cdot \dot{q}^+ > 0$. Following [34], we take solutions of the system to be right continuous and we define the set $\mathcal{S}$ as

$$\mathcal{S} = \{(q, \dot{q}) \mid H(q^-) = 0,\ dH(q^-) \cdot \dot{q}^- < 0\}.$$

We next define an impact map that determines the change in velocity that occurs at the impact event. We let $h : Q \to \mathbb{R}^\nu$ be a smooth function defining the foot/ground contact constraint. For bipeds with point foot contact, the dimension, ν, is two in the planar 2-D case and three in the general 3-D case. For bipeds with extended feet, ν is three for planar bipeds and six in the most general case. The function h

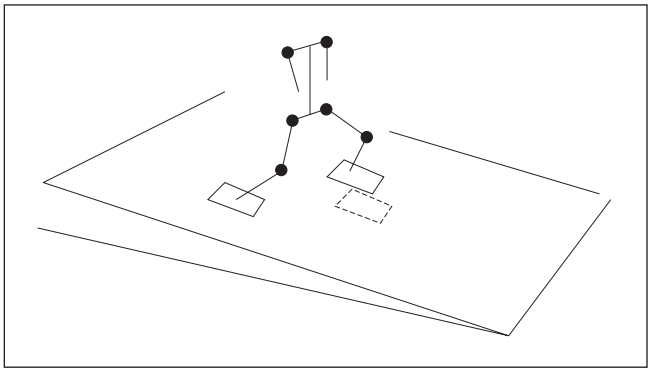

Figure 1. *A general 3-D biped in the single-support phase showing the stance leg (right leg) and swing leg (left leg).*

can be computed using the forward kinematic equations of the robot. Then, as shown in [31], the impact map may be represented as

$$\dot{q}(t^+) = P_q(q(t^-))\,\dot{q}(t^-) \tag{3}$$

and is computed as the $M(q)$-orthogonal projection of $\dot{q}(t^-)$ onto $\{v \in T_qQ |\ dh_i(q)\cdot v = 0,\ \ i = 1, \ldots, \nu\}$.

Putting these previous notions together leads to a hybrid dynamical system

$$\frac{d}{dt}\frac{\partial \mathcal{L}}{\partial \dot{q}} - \frac{\partial \mathcal{L}}{\partial q} = B(q)u, \qquad \text{for } (q(t^-), \dot{q}(t^-)) \notin S \tag{4}$$

$$\left.\begin{aligned} q(t^+) &= q(t^-) \\ \dot{q}(t^+) &= P_q(q(t^-))\,\dot{q}(t^-) \end{aligned}\right\} \quad \text{for } (q(t^-), \dot{q}(t^-)) \in S. \tag{5}$$

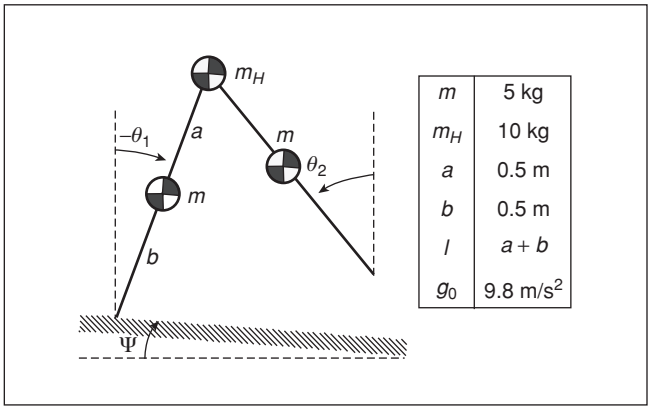

Figure 2. *The compass-gait biped and the parameter values used in our simulations.*

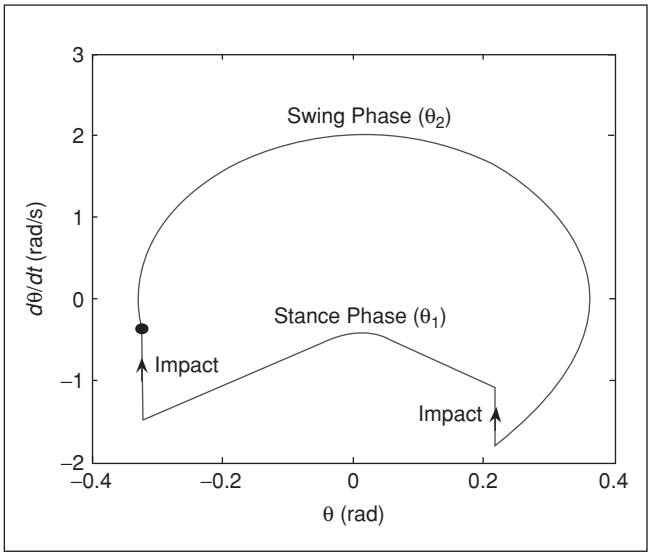

Figure 3. *A typical limit cycle for the compass-gait biped. The circle in this and subsequent figures represents the initial conditions for these variables.*

Example 2.1: For space reasons we will illustrate our results only for the so-called Compass-Gait Biped [7], [8] shown in Figure 2. More complex bipeds are considered in the references, for example [13], [16], [18]. The compass-gait biped is a planar biped with two straight legs, i.e. no knees or torso. As such, it is the simplest biped that can be used to study both passive walking and active control. The configuration variables for the compass-gait biped are taken to be the angles of the stance leg θ_1 and the swing leg θ_2 both with respect to the vertical. The dynamic equations of the compass-gait biped are described by (2), where $q(t) = [q_1(t), q_2(t)]^T = [\theta_1(t), \theta_2(t)]^T$,

$$M(q) = \begin{bmatrix} (m_H + m)\ell^2 + ma^2 & -m\ell b\cos(q_1 - q_2) \\ -m\ell b\cos(q_1 - q_2) & mb^2 \end{bmatrix}$$

$$C(q,\dot{q}) = \begin{bmatrix} 0 & -m\ell b\sin(q_1 - q_2)\dot{q}_2 \\ m\ell b\sin(q_1 - q_2)\dot{q}_1 & 0 \end{bmatrix}$$

$$G(q) = \begin{bmatrix} -(m_H\ell + ma + m\ell)g\sin(q_1) \\ mbg\sin(q_2) \end{bmatrix}$$

$$B = \begin{bmatrix} 1 & 0 \\ 1 & -1 \end{bmatrix}.$$

Impacts occur when the tip of the swing leg contacts the walking surface, i.e. when

$$H(q) = \ell[\cos(q_1 + \psi) - \cos(q_2 + \psi)] = 0, \tag{6}$$

where ψ is the slope of the walking surface. Under the standard assumptions mentioned above, the impact map is given by [8]

$$P(q(t^-))\,\dot{q}(t^-) = \begin{bmatrix} p_{11}^+ & p_{12}^+ \\ p_{21}^+ & p_{22}^+ \end{bmatrix}^{-1} \begin{bmatrix} p_{11}^- & p_{12}^- \\ p_{21}^- & p_{22}^- \end{bmatrix} \dot{q}(t^-), \tag{7}$$

where

$$\begin{aligned} p_{11}^+ &= m\ell(\ell - b\cos(q_1^- - q_2^-)) + ma^2 + m_H\ell^2 \\ p_{12}^+ &= mb(b - \ell\cos(q_1^- - q_2^-)) \\ p_{21}^+ &= -mb\ell\cos(q_1^- - q_2^-),\ \ p_{22}^+ = mb^2 \\ p_{11}^- &= -mab + (m_H\ell^2 + 2ma\ell)\cos(q_1^- - q_2^-) \\ p_{12}^- &= p_{21}^- = -mab,\ \ p_{22}^- = 0\,. \end{aligned}$$

Figure 3 shows a typical passive limit cycle for the compass-gait biped. As the actual trajectory evolves in a four-dimensional space, we show only the phase plot for one leg as it switches from swing phase to stance phase and back to swing phase. Note the two points of discontinuity resulting from the foot/ground impacts.

Control

In this section, we present our main results on control of bipeds described by the hybrid system (4)–(5).

Controlled Symmetries

We first consider the effect of symmetries on Lagrangian dynamics. Let G be a group and let Q be the configuration space of the biped as before. Suppose $\Phi : G \times Q \to Q$ is a group action [31] such that, for all $g \in G$,

$$\mathcal{L}(q, \dot{q}) = \mathcal{L}(\Phi_g(q), T_q\Phi_g(\dot{q})). \tag{8}$$

Equation (8) says that the Lagrangian is invariant under the group action Φ. As a result, the solutions of the Euler-Lagrange equations of motion are also invariant under Φ. Such a Lagrangian system is said to possess a symmetry with respect to the group action Φ. We are interested in deriving control laws that create symmetries with respect to group actions for the hybrid Lagrangian system (4)–(5). For this reason we introduce the notion of controlled symmetry [30], [31] as

Definition 3.1: The hybrid Lagrangian system (4)–(5) is said to possess a controlled symmetry with respect to a group action Φ if, for each $g \in G$, there exists a control input $u = u_g(q, \dot{q})$, which depends on g, such that

$$\frac{d}{dt}\frac{\partial \mathcal{L}}{\partial \dot{q}} - \frac{\partial \mathcal{L}}{\partial q} - B(q)u_g = \frac{d}{dt}\frac{\partial \mathcal{L}_g}{\partial \dot{q}} - \frac{\partial \mathcal{L}_g}{\partial q} \tag{9}$$

$$T\Phi_g(P_q\dot{q}) = P_{\Phi_g}T\Phi_g(\dot{q}), \tag{10}$$

where $\mathcal{L}_g(q, \dot{q}) = \mathcal{L}(\Phi_g(q), T_q\Phi_g(\dot{q}))$.

The importance of a controlled symmetry is that solutions of the hybrid dynamical system are preserved, in a way that we make precise below, under the group action. For our application we are interested in controlled symmetry with $G = SO(3)$ representing the orientation (slope) of the ground relative to an inertial reference frame. Following [31] we let $\Sigma = \{O, \{e_1, e_2, e_3\}\}$ be an inertial reference frame, where the point O is fixed on the ground and we assume the ground is defined by a plane in $\mathbb{R}^3$. Given the coordinates $x \in \mathbb{R}^3$ of a point on the ground, changing the ground slope is an SO(3)-group action $(g, x) \mapsto gx$. Assuming that the contact point for the stance leg is at the origin O of Σ, we define a corresponding action Φ of $SO(3)$ on the configuration space $Q = \mathrm{SO}(3) \times \mathbb{T}^{n-3}$ that maps $(g, q) = (g, (R, r)) \in \mathrm{SO}(3) \times Q$ into Q by

$$\Phi(g, (R, r)) = \Phi_g(R, r) = (gR, r). \tag{11}$$

In [31] we showed that there exists a controlled symmetry for the hybrid Lagrangian model (4)–(5) with respect to the group action (11). Moreover, the control law u_g for $g \in SO(3)$ defining the controlled symmetry is a function only of the potential energy of the robot. Specifically, we have

Theorem 3.2: Let $\eta : [0, T] \to Q$ be a solution trajectory of the hybrid system (4)–(5) corresponding to $u = 0$. Let $g \in \mathrm{SO}(3)$ and define

$$u_g(q) = B^{-1}(q)\frac{\partial}{\partial q}(\mathcal{V}(q) - \mathcal{V}(\Phi_g(q))). \tag{12}$$

Then the trajectory $\Phi_g \circ \eta : [0, T] \to Q$ is a solution for the closed-loop system, that is, for the controlled biped.

See [31] for details of the proof. In particular, Theorem 3.2 tells us that any limit cycle that exists for a passive walker for one ground slope can be reproduced by the active control law (12) on any other ground slope. Also, if $(q_0, \dot{q}_0)$ lies in the basin of attraction of the passive limit cycle, then $(\Phi_g(q_0), T_{q_0}\Phi_g(\dot{q}_0))$ lies in the basin of attraction of the closed-loop system. Thus, we are able to determine the appropriate initial conditions on any slope given one initial condition that leads to a passive gait on one particular slope.

Figure 4 shows the results of the controlled symmetry applied to the compass-gait for three distinct ground slopes. As implied by the theory, the hybrid limit cycles are mapped identically from one slope to another.

Passivity-Based Control

In the previous section, we showed how the notion of controlled symmetry led naturally to a potential energy shaping control that renders any passive limit cycle slope invariant via active feedback control. Although the limit cycles are preserved, the basin of attraction, since it is also preserved, remains rather small. In this section we show how total energy shaping can be used to enlarge the basin of attraction and provide additional robustness. The total energy shaping takes the form of a so-called passivity-based control that we will define below. To begin, we consider an additional control term $\bar{u}$ for the gravity compensation control of the previous section. In other words, we let

$$u = u_g + B^{-1}\bar{u}, \tag{13}$$

where u_g is given by (12) and $\bar{u}$ is an additional control term to be designed. With this definition of u, the equations of motion are, therefore,

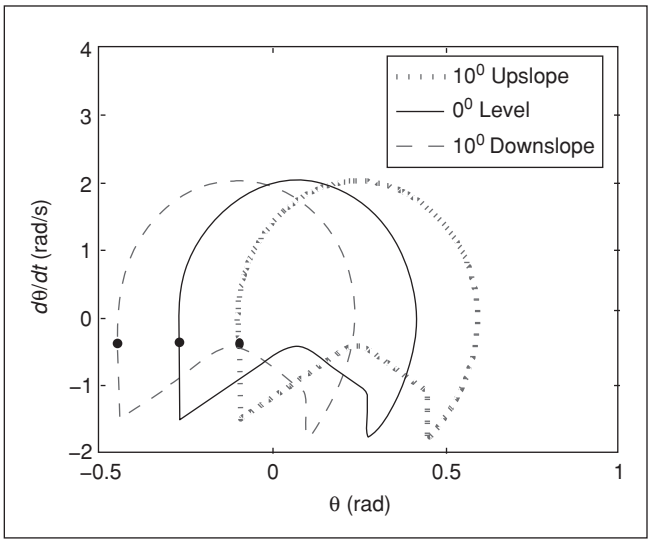

Figure 4. *Three distinct limit cycles for the compass-gait biped on three distinct ground slopes resulting from the application of the control (12) based on the concept of controlled symmetry.*

$$M(q)\ddot{q} + C(q, \dot{q})\dot{q} + G(\Phi_g(q)) = \bar{u}\,. \tag{14}$$

The approach we use to design $\bar{u}$ is based on passivity arguments. We recall the following:

Definition3.3: A dynamical system with input u and output y and state x is said to be passive if there exists a continuously differentiable nonnegative definite scalar function $S(x)$, called a storage function such that

$$\dot{S} = y^T u. \tag{15}$$

Equation (15) can also be written in integral form as

$$S(x(t)) - S(x(0)) = \int_0^t y^T(\sigma)u(\sigma)\,d\sigma\,. \tag{16}$$

Passivity is an important and useful property, as it is related to energy/Lyapunov methods. Equation (16) says, in effect, that the change in storage (energy) is due only to that supplied by the external input u.

It is well known [33] that the robot dynamic model (14) defines a passive system with input $\bar{u}$, output $\dot{q}$ and total energy (kinetic plus potential),

$$E = \frac{1}{2}\dot{q}^T M(q)\dot{q} + V(\Phi_g(q))\,, \tag{17}$$

as the storage function, since

$$\dot{E} = \bar{u}^T\dot{q}$$

follows from the skew-symmetry of $\dot{M} - 2C$ by direct calculation.

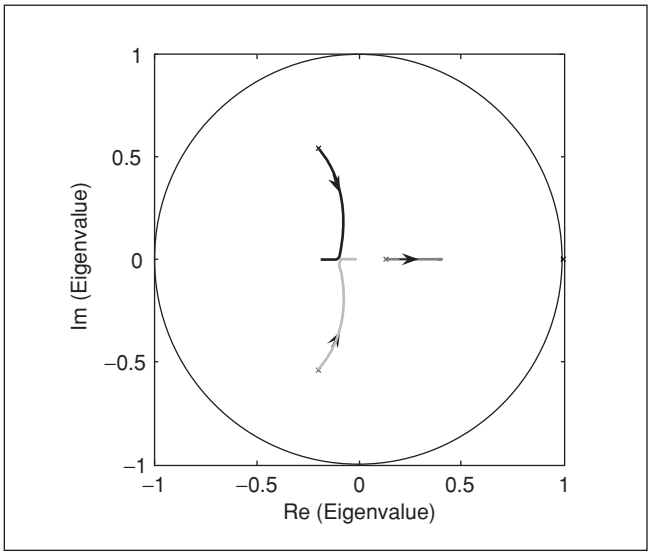

Figure 5. *Locus of the eigenvalues of the linearized Poincaré map for the compass-gait biped with passivity-based control law (20) as the gain k is varied from 0 to 2.*

To utilize the passivity property of robot dynamics in our application, it turns out to be most useful to take as a storage function

$$S = \frac{1}{2}(E - E_{ref})^2 \tag{18}$$

rather than the energy E alone, where E_{ref} is a reference value corresponding to the energy of the biped along the limit cycle trajectory of the system corresponding to a fixed ground slope. Note that S is identically zero on the limit cycle trajectory and nonnegative away from the limit cycle.

Suppose now that E_{ref} is constant. Then, a simple calculation shows that

$$\dot{S} = (E - E_{\text{ref}})\dot{E} = (E - E_{\text{ref}})\dot{q}^T\bar{u}\,. \tag{19}$$

With this storage function, the system is therefore passive with respect to input $\bar{u}$ and output $y = (E - E_{ref})\dot{q}$. This suggests that we choose the control input as

$$\bar{u} = -ky = -k(E - E_{\text{ref}})\dot{q}\,, \tag{20}$$

where $k > 0$ is a fixed gain. Substituting (20) into (19) yields

$$\dot{S} = -k||y||^2 = -2k||\dot{q}||^2 S \le 0\,. \tag{21}$$

Proposition 3.4: Suppose there is a constant $\alpha > 0$ such that $||\dot{q}(t)||^2 \ge \alpha$ for all $0 \le t < T_1$, where T_1 is the time of first impact of the swing foot with the ground. Then

$$S(t) \le S(0)e^{-2k\alpha t} \quad \text{for } 0 \le t < T_1\,. \tag{22}$$

Proof: Under the above assumption

$$\dot{S}(t) \le -2k||\dot{q}||^2 S \le -2k\alpha S, \tag{23}$$

and so the result follows from the comparison principle ([15, pg. 102]).

Proposition 3.4 implies that the total energy of the biped will converge exponentially toward the reference energy between impacts. At the impact, the storage function will exhibit a jump discontinuity. Therefore, in order for the energy to converge to its reference value, the sequence of discrete points defined by the jumps must also converge to zero. This latter convergence can be investigated by computing a so-called Poincaré map that maps the values of the joint angles and joint velocities from one step to the next.

If we denote by $x_\ell := (q_\ell^T(t^+), \dot{q}_\ell^T(t^+))^T$ the joint angles and velocities at the beginning of step ℓ, i.e., just after the foot/ground impact, then, the hybrid system (4)–(5) defines a discrete map

$$x_{\ell+1} = P(x_\ell) \tag{24}$$

known as a Poincaré map. Existence of a limit cycle trajectory is then implied by a fixed point of this mapping, i.e. a vector x^* such that

$$x^* = P(x^*)\,. \tag{25}$$

Asymptotic stability of the Poincaré map then implies (local) asymptotic orbital stability of the limit cycle and, hence, convergence of the energy to the reference energy. To determine asymptotic stability of the Poincaré map (24), we may calculate the linearized approximation around the limit cycle using the hybrid sensitivity analysis techniques described in [10]. Figure 5 shows a plot of the eigenvalues of the linearized approximation of the Poincaré map (24) for the compass-gait biped as a function of the gain k in the control law (20). Since these eigenvalues are inside the unit disk, the Poincaré map is indeed locally asymptotically stable. This is indeed confirmed by Figure 6 showing the storage function for $k = 1$.

Basin of Attraction and Rate of Convergence

The Basin of Attraction of the limit cycle is the set of initial conditions in state space such that trajectories starting at these initial conditions converge asymptotically to the limit cycle. Since the state space is four dimensional and the equations of motion highly nonlinear, the basin of attraction is difficult to characterize precisely. Typically, one finds a narrow band of initial conditions around the limit cycle where trajectories converge. One may consider the relative stability of the limit cycle by looking at the eigenvalues of the linearized Poincaré map. Roughly speaking, the smaller the modulus of eigenvalues are, the more robust the limit cycle is to disturbances and unmodeled dynamics and the quicker the trajectory will converge to the limit cycle. Convergence to the limit cycle can also be characterized by the number of steps required to converge to within a given error band around the limit cycle.

Figures 7 and 8 show trajectories with and without the passivity-based control (20). In Figure 7 a point previously outside the basin of attraction is captured by the addition control term $\bar{u}$. While the precise change in the basin of attraction is difficult to characterize, the total energy control seems to increase the basin for a range of gains, k. Figure 8 shows that the rate of convergence of the trajectory to the limit cycle is also greatly improved by the addition of the passivity-based control term $\bar{u}$.

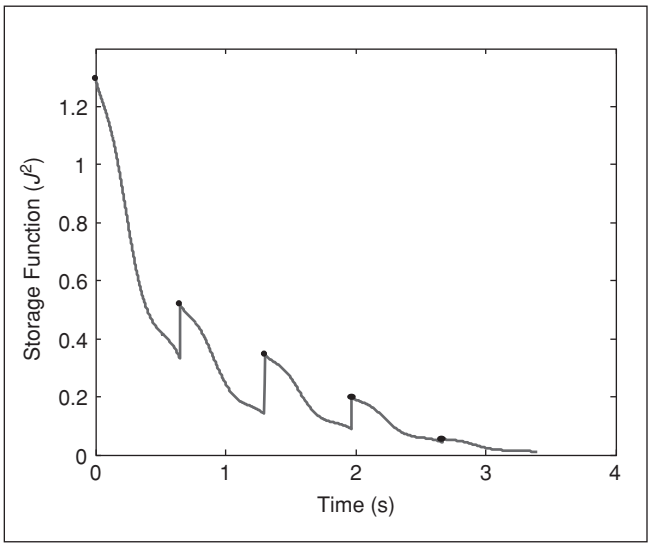

Figure 6. *Value of the storage function versus time using the passivity-based control (20) with $k = 0.5$. S decreases exponentially between foot/ground impacts and the values at the impacts also decrease to zero as a consequence of asymptotic stability of the Poincaré map.*

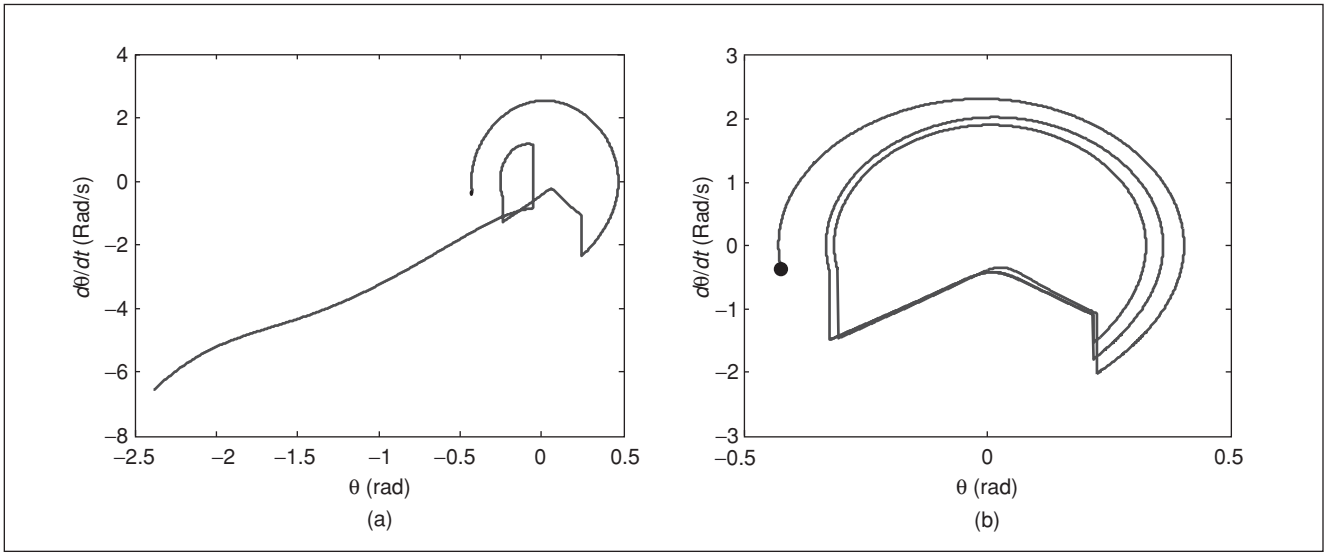

Figure 7. *Starting from the same initial conditions, the response in (a) without the passivity-based control law (20) is unstable; the response in (b) with the passivity-based control law (20) converges to the limit cycle showing that the initial condition is now contained within the basin of attraction.*

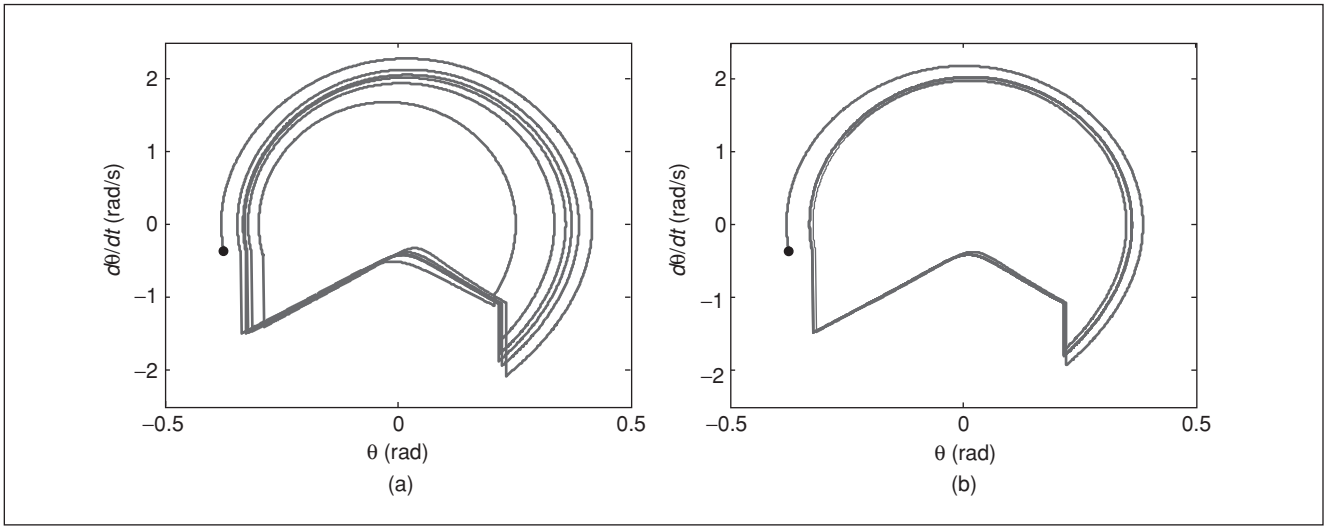

Figure 8. *Starting from the same initial conditions, the convergence to the limit cycle in (a) without the passivity-based control law (20) is slower than the convergence to the limit cycle in (b) with the passivity-based control with (20).*

Slope Variation and External Disturbances

As a further illustration of the robustness enhancement of the passivity-based control, we show the performance of the system when the slope exhibits a sudden change and when the robot is subject to a constant disturbance torque. The control input is always determined by the so-called local slope, which is the ground slope at the stance leg. The local slope can be determined by the two-point contact condition, which occurs at the moment of contact of the swing foot with the ground as shown in Figure 9. Thus for a discrete slope change there are generically two steps during which an error in the perceived ground slope occurs. Figure 10(a) shows that without the total energy control, the robot is not able to maintain a stable gait. Figure 10(b) shows that, with the addition of the total energy based control $\bar{u}$, the biped successfully makes the transition between slopes.

Figure 11 shows the effect of a 1-Nm disturbance torque added to each joint of the biped. This disturbance is sufficient to cause the biped to fall without the total energy shaping control whereas stability is maintained when the total energy shaping control is used.

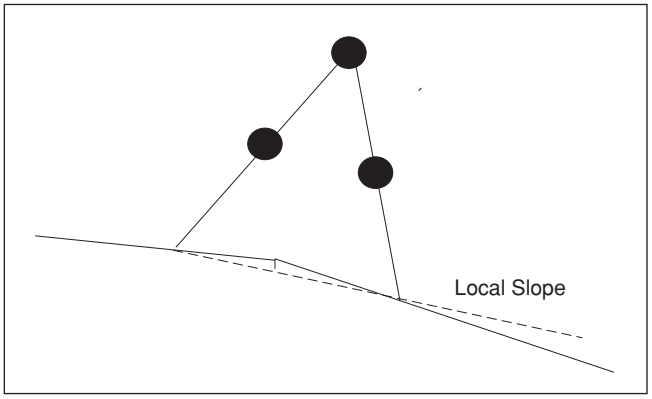

Figure 9. *Slope change from a 3° down slope to an 8° down slope. The local slope, determined by the two-point contact, is used in the controlled symmetry and passivity-based control to achieve robustness to the slope change.*

Trajectory Time Scaling

Trajectory time scaling in robot control has been used previously to address several problems in manipulator control, such as time-optimal control along a given path [2], [25], [26], actuator saturation [5], control of swimming robots [24], and others [11]. In this section we consider the use of trajectory time scaling for the problem of regulating walking speed in bipedal locomotion. As in other problems involving walking, the foot/ground impacts that introduce velocity discontinuities between steps must be taken into account when time scaling the biped trajectories. This distinguishes the results here from the results in the above references. The results we present here are taken from [13].

Consider again the n-DOF Lagrangian system (14). For notational simplicity we will simply take $g = I$ the identity element of $SO(3)$. Let $\phi : \mathbb{R}^+ \to \mathbb{R}^+$ be a continuously differentiable and monotonic map such that $\phi(0) = 0$ and $\dot{\phi}(t) > 0$ for $t \in \mathbb{R}^+$. We refer to $t' = \phi(t)$ as scaled time and we define scaled coordinates, $q_{sc}(t)$ as

$$q_{sc}(t) = q(\phi(t)) = q(t'). \tag{26}$$

The scaled velocity and acceleration are then given by

$$\dot{q}_{sc}(t) = \frac{\partial q(\phi)}{\partial \phi}\frac{d\phi}{dt} = \dot{q}(t')\dot{\phi} \tag{27}$$

$$\ddot{q}_{sc}(t) = \ddot{q}(t')\dot{\phi}^2 + \dot{q}(t')\ddot{\phi}. \tag{28}$$

In terms of the scaled trajectory $q_{sc}(t)$, we can express (14) as

$$M(q_{sc}(t))\ddot{q}_{sc}(t) + C(q_{sc}(t), \dot{q}_{sc}(t))\dot{q}_{sc}(t) + G(q_{sc}(t)) = \bar{u}_{sc}(t). \quad (29)$$

Substituting (26)–(28) into (29) and using (14), we have

$$\begin{aligned}\bar{u}_{sc}(t) &= M(q(t'))[\ddot{q}(t')\dot{\phi}^2 + \dot{q}(t')\ddot{\phi}] \\ &\quad + C(q(t'), \dot{q}(t')\dot{\phi})\dot{q}(t')\dot{\phi} + G(q(t')) \\ &= \dot{\phi}^2[M(q(t'))\ddot{q}(t') + C(q(t'), \dot{q}(t'))\dot{q}(t')] \\ &\quad + M(q(t'))\dot{q}(t')\ddot{\phi} + G(q(t')) \\ &= \dot{\phi}^2\bar{u}(t') + (1-\dot{\phi}^2)G(q(t')) \\ &\quad + M(q(t'))\dot{q}(t')\ddot{\phi},\end{aligned}$$

where the second equality follows from the fact that $C(q, \star)\star$ is quadratic in $\star$. We have thus shown the following.

Proposition 3.5: Suppose that control input $\bar{u}_0(t)$ and initial conditions $(q_0(0), \dot{q}_0(0))$ yield the solution trajectory $(q_0(t), \dot{q}_0(t))$ for $0 \le t \le T$. Then the control input

$$\begin{aligned}\bar{u}_{sc}(t) &= \dot{\phi}^2\bar{u}_0(t') + (1-\dot{\phi}^2)G(q_0(t')) \\ &\quad + M(q_0(t'))\dot{q}_0(t')\ddot{\phi} \quad (30)\end{aligned}$$

yields the scaled solution trajectory $(q_{sc}(t), \dot{q}_{sc}(t))$ for $0 \le t \le \phi^{-1}(T)$.

Special Case: Constant Time Scaling

In the special case that $t' = \phi(t) = \lambda t$, i.e., the scaled time is a constant multiple of real time, then the control law (30) reduces to

$$\bar{u}_{sc}(t) = \lambda^2\bar{u}_0(\lambda t) + (1-\lambda^2)G(q_0(\lambda t)) \quad (31)$$

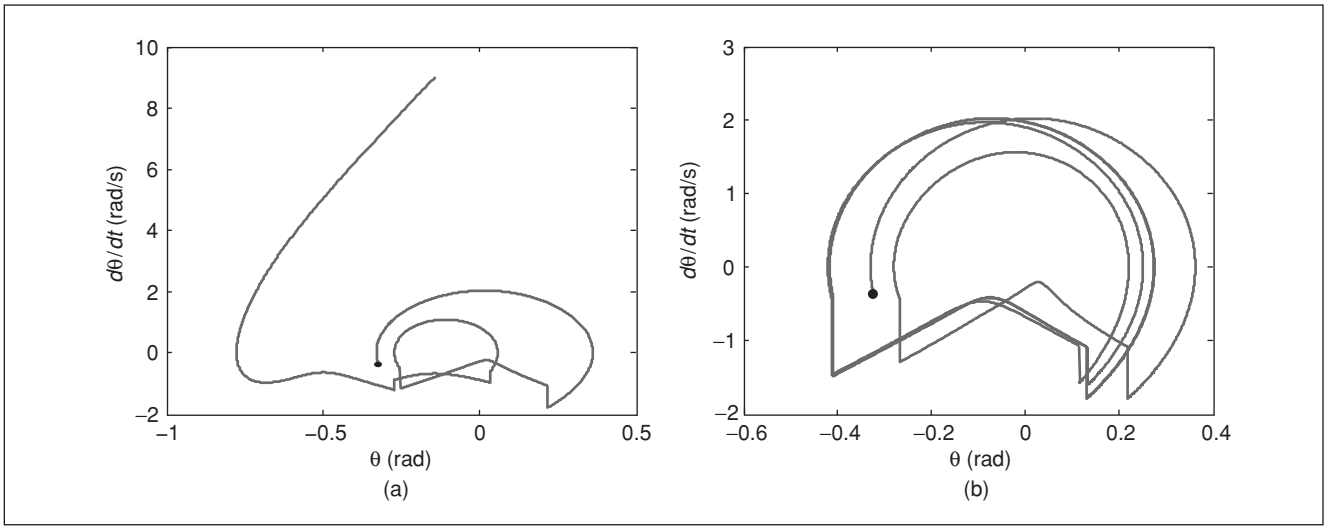

Figure 10. *Closed loop trajectory on terrain with slope change from 3° down slope to 8° down slope. In (a) without the passivity-based control law (20), the abrupt change in slope causes the biped to fall. In (b) with the passivity-based control law (20), the biped successfully negotiates the change in slope.*

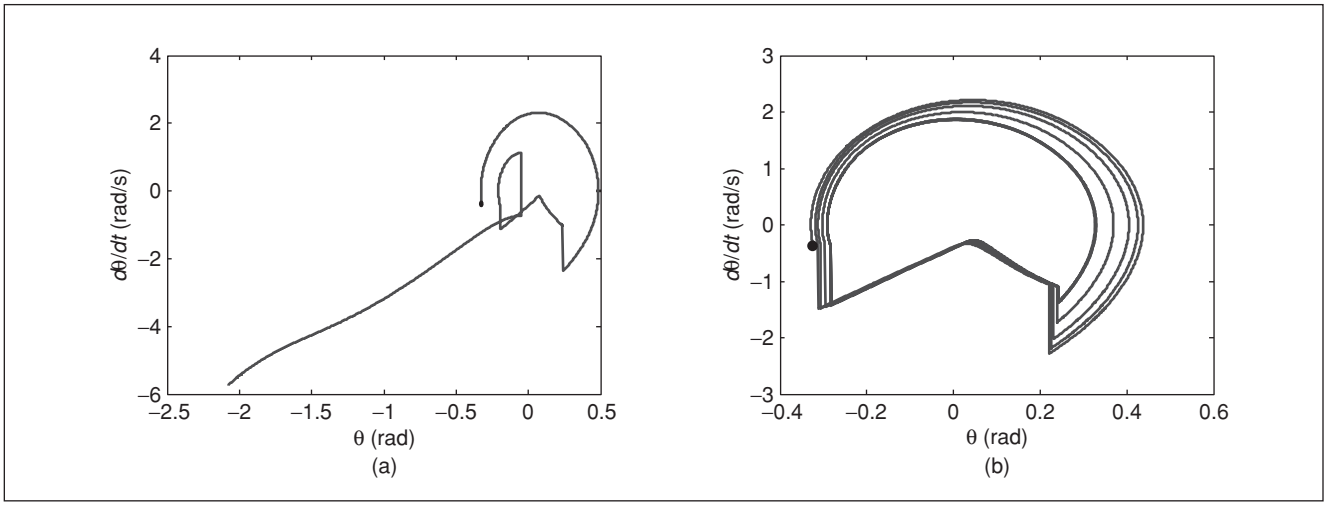

Figure 11. *Trajectories with a 1-Nm disturbance torque at each joint. In (a) without the passivity-based control law (20), the robot falls. In (b) with the passivity-based control law (20), the trajectory remains close to the limit cycle despite the disturbance torque.*

and results in trajectories that scale the position, velocity, and accelerations as

$$
\begin{aligned}
q_{sc}(t) &= q_0(\lambda t) \\
\dot{q}_{sc}(t) &= \lambda \dot{q}_0(\lambda t) \\
\ddot{q}_{sc}(t) &= \lambda^2 \ddot{q}_0(\lambda t)
\end{aligned}
$$

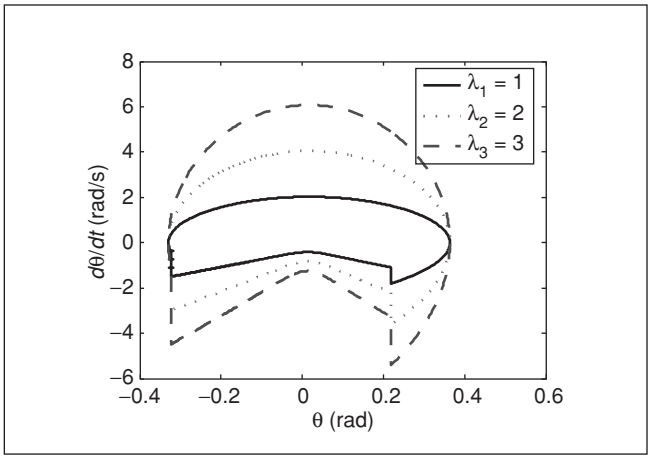

Figure 12. *Limit cycles for the compass-gait biped under constant time-scaling control $\phi(t) = \lambda t$ with various values of parameter λ.*

for $0 \le t \le \phi^{-1}(T) = T/\lambda$ with initial condition $(q_{sc}(0), \dot{q}_{sc}(0)) = (q_0(0), \lambda \dot{q}_0(0))$.

Note that the additional control term $(1 - \lambda^2)G(q_0(\lambda t))$ is, once again, simply a potential energy shaping control that cancels the effect of normal gravity $G(q_0)$ on the system dynamics and substitutes the effect of scaled gravity $\lambda^2 G(q_0)$.

To apply the above time-scaling result to regulate walking speed in biped locomotion, we must take into account impacts resulting from foot/ground contact. Under linear time scaling $\phi(t) = \lambda t$, we have $\dot{q}_{sc}(t') = \lambda \dot{q}_0(t')$. Consequently,

$$
\begin{aligned}
\dot{q}_{sc}(t^+) = \lambda \cdot \dot{q}_0(t^+) &= \lambda \cdot P(q_0(t^-))\dot{q}_0(t^-) \\
&= P(q_0(t^-)) \cdot \lambda \dot{q}_0(t^-) \\
&= P(q_{sc}(t^-))\dot{q}_{sc}(t^-) \qquad (32)
\end{aligned}
$$

and

$$
q_{sc}(t^+) = \lambda q_0(t^+) = \lambda q_0(t^-) = q_{sc}(t^-),
$$

so the impact event scales the impact velocities linearly by the constant λ, matching the scaling of the rest of the trajectory and effectively stretching or shrinking the entire limit cycle.

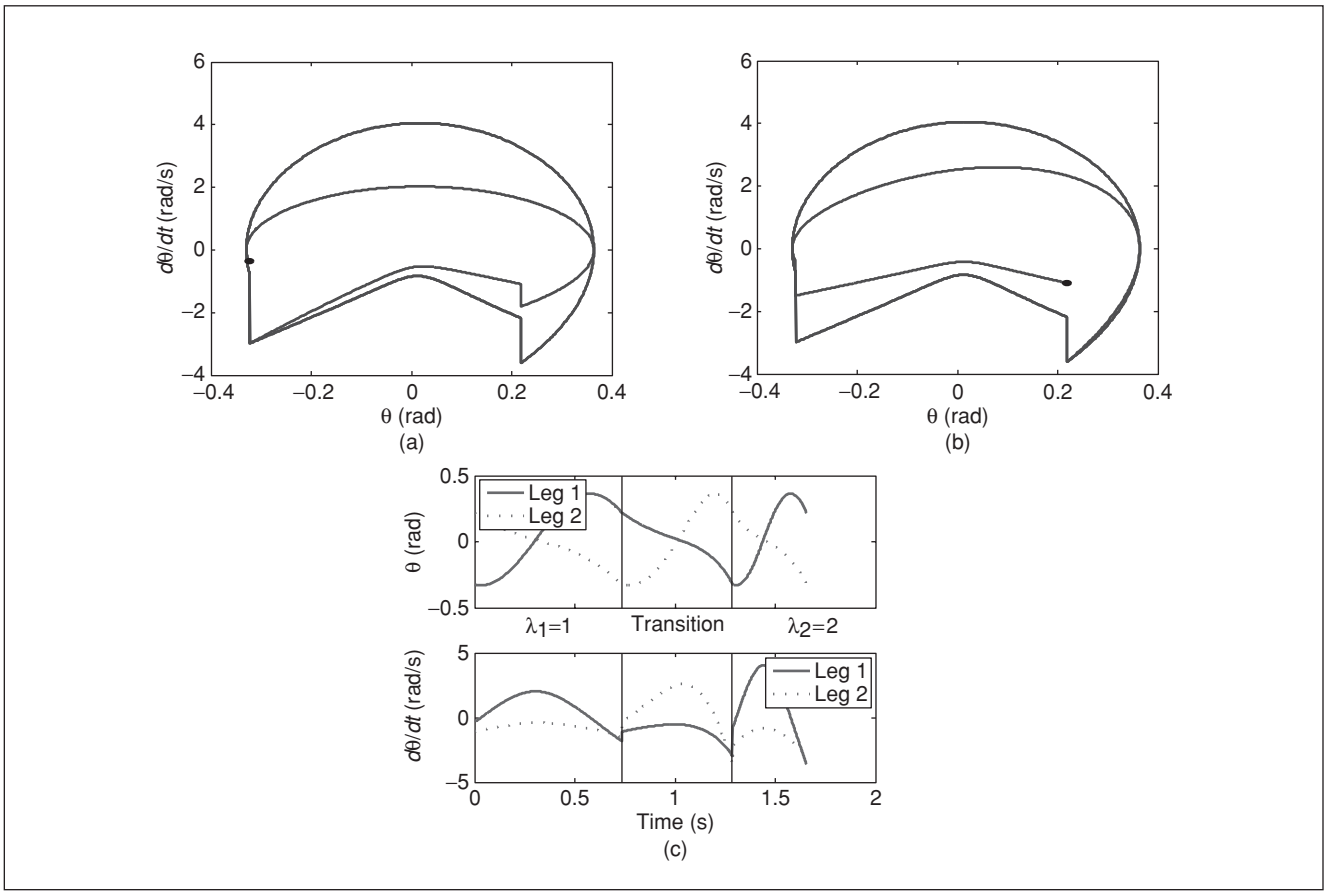

Figure 13. *Compass-gait biped trajectories showing a transition from the original limit cycle ($\lambda_1 = 1$) to a time-scaled limit cycle described by $\lambda_2 = 2$. (a), (b) Phase portrait of swing and stance legs and (c) joint trajectories.*

Gait Transition

Under variable time scaling $\phi(t)$, a similar expression for the velocity change at impact holds as in the case of constant scaling. However, since the scaling is nonuniform, the post-impact final velocity $\dot{q}_{sc}(t^+)$ is not the same as the initial velocity of the trajectory $\dot{q}_{sc}(0)$. Instead, the final velocity serves as the initial condition of a new limit cycle with a velocity different from the original. This property enables us to transition between stable walking gaits of different periods. In this section, we develop a time-scaling function to transition between limit cycles in a single step.

Consider the task of making a transition from a limit cycle described by constant time-scaling function $\phi_1(t) = \lambda_1 t$ and another limit cycle described by $\phi_2(t) = \lambda_2 t$. Clearly, $\dot{\phi}_i(t) = \lambda_i$ for each of these limit cycles. To move from one to the other, we construct a time-scaling function $\phi_\Delta(t)$ whose derivative is equal to λ_1 at the beginning of the step and equal to λ_2 at the end of the step. That is,

$$\begin{aligned} \phi_\Delta(0) &= 0 \quad \phi_\Delta(t_F) = T \\ \dot{\phi}_\Delta(0) &= \lambda_1 \quad \dot{\phi}_\Delta(t_F) = \lambda_2 \end{aligned}$$

where t_F is the desired time (in seconds) of the end ground impact, which we are free to choose provided $\dot{\phi}_\Delta(t) > 0$ for $0 \le t \le t_F$. These four conditions are satisfied by the cubic polynomial given by

$$\begin{aligned} \phi_\Delta(t) =& \lambda_1 t + \left(\frac{3T}{t_F^2} - \frac{2\lambda_1 + \lambda_2}{t_F} \right) t^2 \\ &+ \left(-\frac{2T}{t_F^3} + \frac{\lambda_1 + \lambda_2}{t_F^2} \right) t^3 . \end{aligned}$$

Remark 3.6: We have shown that any path in configuration space $q_0(t)$, $0 \le t \le T$, that represents the position portion of a limit cycle of period T can be exactly followed at any constant scaled velocity $\lambda \dot{q}_0(t)$ using the control law (31) resulting in a limit cycle of period T/λ. Moreover, we have shown how to transition between limit cycles of distinct periods in a single step using a cubic polynomial time-scaling function. This is a general result, independent of the particular control generating the original limit cycle.

Figure 12 shows limit cycles for the compass-gait biped for various values of λ. We see from the figures that the initial and final values of the configuration variables θ_1, θ_2 are identical while the velocities $\dot{\theta}_1, \dot{\theta}_2$ vary with selection of the parameter λ. Figure 13(a) is a phase portrait of the compass gait biped under our time-scaling control transitioning from the passive limit cycle described by $\lambda_1 = 1$ to a limit cycle described by $\lambda_2 = 2$ with varying time scaling $\phi_\Delta(t)$ and transition time $t_F = 0.5$ seconds. Figure 13(c) shows the trajectories of the system as it moves from the passive limit cycle ($\lambda_1 = 1$) to the $\lambda_2 = 2$ limit cycle.

Conclusions

In this article, we have shown how to design energy-based and passivity-based control laws that exploit the existence of passive walking gaits to achieve walking on different ground slopes, to increase the size of the basin of attraction and robustness properties of stable limit cycles, and to regulate walking speed. Many of the results presented here for the compass gait are equally applicable to bipeds with knees and a torso. See [13], [29] for some examples. There are several interesting ways to explore extensions to these results. Practical considerations such as actuator saturation, ground reaction forces, and ground friction need to be addressed. The problem of foot rotation introduces an underactuated phase into the walking gait, which greatly challenges the application of energy shaping ideas. For walking in 3-D, finding purely passive limit cycles, which is the first step in applying our energy control results, may be difficult. In [1] it was shown how ideas of geometric reduction can be used to generate 3-D stable gaits given only 2-D passive limit cycles. This work greatly expands the applicability of the results presented here.

Acknowledgments

This research was partially supported by the National Science Foundation under Grant CMS-0510119. The authors would like to acknowledge the contributions of Francesco Bullo and Gagandeep Bhatia to some of the earlier work on energy shaping control surveyed here. We would also like to thank the reviewers for their very constructive comments and suggestions.

Keywords

Passivity-based control, bipedal locomotion, passive walking, group action, symmetry, limit cycle, potential energy shaping, trajectory time scaling.

References

[1] A.D. Ames, R.D. Gregg, E.D.B. Wendel, and S. Sastry, "Towards the geometric reduction of controlled three-dimensional robotic bipedal walkers," in *Proc. Workshop Lagrangian Hamiltonian Methods Nonlinear Control*, Nagoya, Japan, July 2006, pp. 117–124.

[2] J.E. Bobrow, S. Dubowsky, and J.S. Gibson, "Time-optimal control of robotic manipulators along specified paths," *Int. J. Robot. Res.,* vol. 4, no. 3, pp. 3–17, 1985.

[3] C. Chevallereau, "Time-scaling control for an underactuated biped robot," *IEEE Trans. Robot. Automat.*, vol 19, no. 2, pp. 362–368, Apr. 2003.

[4] S.H. Collins, M. Wisse, and A. Ruina, "A three-dimensional passive-dynamic walking robot with two legs and knees," *Int. J. Robot. Res.*, vol. 20, no. 7, pp. 607–615, 2001.

[5] O. Dahl and L. Nielsen, "Torque-limited path following by on-line trajectory time scaling," *IEEE Trans. Robot. Automat.*, vol. 6, no. 5, pp. 554–561, 1990.

[6] M. Garcia, A. Chatterjee, A. Ruina, and M. Coleman, "The simplest walking model: Stability, complexity, and scaling," *ASME J. Biomechan. Eng.*, vol. 120, no. 2, pp. 281–288, 1998.

[7] A. Goswami, B. Espiau, and A. Keramane, "Limit cycles in a passive compass gait biped and passivity-mimicking control laws," *Autonomous Robots*, vol. 4, no. 3, pp. 273–286, 1997.

[8] A. Goswami, B. Thuilot, and B. Espiau, "A study of the passive gait of a compass-like biped robot: Symmetry and chaos," *I. J. Robot. Res.*, vol. 17, no. 12, pp. 1282–1301, 1998.
[9] J.W. Grizzle, G. Abba, and F. Plestan, "Asymptotically stable walking for biped robots: analysis via systems with impulse effects," *IEEE Trans. Automat. Contr.*, vol. 46, no. 1, pp. 51–64, Jan. 2001.
[10] I.A. Hiskens, "Stability of Hybrid System Limit Cycles: Application to the Compass Gait Biped Robot," in *Proc. 40th IEEE Conf. Decision Control*, Orlando, FL, Dec. 2001, pp. 774–779.
[11] J.M. Hollerbach, "Dynamic scaling of manipulator trajectories," *ASME J. Dyn. Syst., Meas., & Contr.*, vol. 106, pp. 102–106, 1984.
[12] J.K. Holm, "Control of passive dynamic robots using artificial potential energy fields," M.S. thesis, ECE Dept., Univ. Illinois Urbana-Champaign, Illinois, 2005.
[13] J.K. Holm, D.J. Lee, and M.W. Spong, "Time scaling for speed regulation in bipedal locomotion," in *Proc. IEEE Int. Conf. Robotics Automation*, Rome, Italy, Apr., 2007, pp. 3603–3608.
[14] Y. Hurmuzlu and G. Moskowitz, "The role of impact in the stability of bipedal locomotion," *Dyn. Stability Syst.*, vol. 1, no. 3, pp. 217–234, 1986.
[15] H. Khalil, *Nonlinear Systems*, 3rd ed. Englewood-Cliffs, NJ: Prentice-Hall, 2002.
[16] N. Khraief, N.K. M'Sirdi, and M.W. Spong, "Nearly passive dynamic walking of a biped robot," in *Proc. European Control Conf.*, Cambridge, U.K., 1–4 Sept. 2003.
[17] A.D. Kuo, "Stabilization of lateral motion in passive dynamic walking," *Int. J. Robot. Res.*, vol. 18, no. 9, pp. 917–930, 1999.
[18] O. Licer, N. M'Sirdi, and N. Manamanni, "Stable periodic gaits of n-link biped robot in three dimensional space," in *Proc. 8th Int. IFAC Symp.Robot Control*, Bologna, Italy, Sep. 2006.
[19] J.E. Marsden and T.S. Ratiu, *Introduction to Mechanics and Symmetry*, 2nd ed. New York: Springer-Verlag, 1999.
[20] T. McGeer, "Passive dynamic walking," *Int.J. Robot. Res.*, vol. 9, no. 2, pp. 62–82, 1990.
[21] T. McMahon, "Mechanics of locomotion," *Int. J. Robot. Res.*, vol. 3, no. 2, pp. 4–28, 1984.
[22] H. Ohta, M. Yamakita, and K. Furuta, "From passive to active dynamic walking," in *Proc. IEEE Conf. Decision Control*, Phoenix, AZ, Dec. 1999, pp. 3883–3885.
[23] J. Ostrowski, "Computing reduced equations for robotic systems with constraints and symmetries," *IEEE Trans. Robot. Automat.*, vol. 15, no. 1, 1999.
[24] S. Saimek and P.Y. Li, "Motion planning and control of a swimming machine," *Int. J. Robot. Res.*, vol. 23, no. 1, pp. 27–54, 2004.
[25] Z. Shiller and H.H. Lu, "Computation of path constrained time optimal motions with dynamic singularities," *ASME J. Dyn. Syst., Meas., & Contr.*, vol. 114, pp. 34–40, 1992.
[26] K.G. Shin and N.D. McKay, "Minimum-time control of robotic manipulators with geometric path constraints," *IEEE Trans. Automat. Contr.*, vol. 30, no. 6, pp. 531–541, 1985.
[27] M.W. Spong, "Bipedal locomotion, robot gymnastics, and robot air hockey: A rapprochement," in *Proc. TITech COE/Super Mechano-Systems Workshop*, Tokyo, Japan, Feb. 1999, pp. 34–41.
[28] M.W. Spong, "Passivity based control of the compass gait biped," in *Proc. IFAC Triennial World Congr.*, Beijing, China, vol. 3, July 1999, pp. 19–23.
[29] M.W. Spong, "The passivity paradigm in bipedal locomotion," in *Proc. CLAWAR*, Madrid, Spain, Sept. 2004, pp. 775–786.
[30] M.W. Spong and F. Bullo, "Controlled symmetries and passive walking," in *Proc. IFAC Triennial World Congr.*, Barcelona, Spain, July, 2002.
[31] M.W. Spong and F. Bullo, "Controlled symmetries and passive walking," *IEEE Trans. Automat. Contr.,* vol. 50, no. 7, pp. 1025–1031, July, 2005.
[32] M.W. Spong and G. Bhatia, "Further results on control of the compass gait biped," in *Proc. IROS 2003*, Las Vegas, Nevada, 27–30 Oct. 2003, pp. 1933–1938.
[33] M.W. Spong, S. Hutchinson and M. Vidyasagar, *Robot Modeling and Control*. Hoboken, NJ: Wiley, 2006.
[34] E.R. Westervelt, J.W. Grizzle, C. Chevallereau, J.H. Choi, and B. Morris, *Feedback Control of Dynamic Bipedal Robot Locomotion*. London, U.K.: CRC Press, 2007.

Mark W. Spong received the B.A. degree, magna cum laude and Phi Beta Kappa, in mathematics and physics from Hiram College, Hiram, Ohio in 1975, the M.S. degree in mathematics from New Mexico State University in 1977, and the M.S. and D.Sc. degrees in systems science and mathematics in 1979 and 1981, respectively, from Washington University in St. Louis. Since 1984, he has been at the University of Illinois at Urbana-Champaign, where he is currently a Donald Biggar Willett Distinguished Professor of Engineering, Professor of Electrical and Computer Engineering, and Director of the Center for Autonomous Engineering Systems and Robotics. He is Past President of the IEEE Control Systems Society and a Fellow of the IEEE. His main research interests are in robotics, mechatronics, and nonlinear control theory. He has published more than 200 technical articles in control and robotics and is coauthor of four books. His recent awards include the Senior U.S. Scientist Research Award from the Alexander von Humboldt Foundation, the Distinguished Member Award from the IEEE Control Systems Society, the John R. Ragazzini and O. Hugo Schuck Awards from the American Automatic Control Council, and the IEEE Third Millennium Medal.

Jonathan K. Holm is a Ph.D. student in the Department of Electrical and Computer Engineering at the University of Illinois at Urbana-Champaign. He received the B.S. degree in engineering from Baylor University and the M.S. degree in electrical engineering from the University of Illinois at Urbana-Champaign. His interests include human and robot locomotion—nonlinear control, dynamics, and biomechanics.

Dongjun Lee received the B.S. degree in mechanical engineering from Korea Advanced Institute of Science and Technology (KAIST), Taejon, Korea in 1995, the M.S. degree in automation and design from KAIST, Seoul, Korea in 1997, and the Ph.D. degree in mechanical engineering from the University of Minnesota at Twin Cities in 2004. From 2004 to 2006, he was a postdoctoral research fellow with the Coordinated Science Laboratory at the University of Illinois at Urbana-Champaign. He is currently an assistant professor with the Department of Mechanical, Aerospace, and Biomedical Engineering at the University of Tennessee-Knoxville. His main research interests are dynamics and control of mechatronic and robotic systems with particular emphasis on multirobot systems, teleoperation, haptics, and geometric control theory. He is a Member of the IEEE and was a recipient of 2002-2003 Doctoral Dissertation Fellow of the University of Minnesota.

Address for correspondence: Mark W. Spong, Coordinated Science Laboratory, University of Illinois at Urbana-Champaign, 1308 W. Main Street, Urbana, IL 61801 USA. E-mail: mspong@uiuc.edu.